Coupled-Channel and Microscopic Analysis of the "Quasi-Elastic" and "Quasi-Inelastic" Ti(^{3}He,^{3}H) Data*

J. J. WESOLOWSKI AND ERVIN H. SCHWARCZ†
Lawrence Radiation Laboratory, University of California, Livermore, California

AND

P. G. ROOS‡ AND C. A. LUDEMANN§
Oak Ridge National Laboratory, Oak Ridge, Tennessee

(Received 25 October 1967; revised manuscript received 2 February 1968)

The (^{3}He,^{3}H) reaction differential cross sections for all the stable Ti isotopes have been measured at a ^{3}He bombarding energy of 24.6 MeV. Information about the strength and shape of the isobaric-spin-dependent potential is obtained from a comparison of the "quasi-elastic" data, with theoretical angular distributions obtained using a coupled-channel formalism. These calculations are compared with the results of calculations using the less exact distorted-wave Born-approximation (DWBA) formalism. The shape and strength of the effective nucleon-nucleon interaction in nuclear matter is obtained from comparisons of the data with calculations made using a microscopic model. The results are compared with those obtained from an analysis of (p,n) data. Finally, an analysis of "quasi-inelastic" transitions to excited isobaric states is made in terms of the collective-model description of inelastic scattering.

I. INTRODUCTION

MEASUREMENTS of the differential cross sections for the (^{3}He,^{3}H) reaction on all the stable Ti isotopes have been made for a ^{3}He bombarding energy of 24.6 MeV. This charge-exchange reaction is expected to be quite similar to the (p,n) charge-exchange reaction, but is more tractable to experimental study. Although angular distributions were measured for a number of final states in the residual nuclei, this paper will be concerned primarily with the "quasi-elastic" yields to the isobaric analogs of the target ground states.

The measurements were undertaken in part to study the variation of the Coulomb displacement energy, and hence the charge radius, as a function of neutron excess for all the isotopes of one element. Previous measurements and calculations for other isotopes in this mass region indicate that the charge radius increases more slowly than $A^{1/3}$ as the neutron excess increases.[1] The measurements on the Ti isotopes show quite similar results.

It was also of interest to measure the ground-state analog cross sections as a function of neutron excess. Theoretical formulations of the "quasi-elastic" scattering process predict that the cross section is directly proportional to $(N-Z)$. However, recent measurements of the "quasi-elastic" (p,n) cross sections from the Ti isotopes show that the odd isotopes depart strongly from this prediction.[2] The (^{3}He,^{3}H) measurements also show an odd-even effect, although not as pronounced as in the (p,n) case. The above results have been discussed in an earlier paper.[3]

The analog transition can be interpreted as arising from an isospin or symmetry term in the optical-model potential.[4] An exact solution of the Schrödinger equation using such a potential results in a set of coupled equations.[5] By fitting the angular distributions with the predicted cross sections from this formalism, one can obtain information on the shape and strength of this symmetry term. Results obtained using this interpretation are discussed in Sec. III, and are compared with the results of calculations using the less exact DWBA approach in Sec. IV.

One can also treat the charge-exchange reaction in a manner which is microscopic compared to the optical-model formalism, i.e., one in which the interaction causing the transition is taken to be a sum of two-body forces between the projectile and target nucleons.[6] Results of calculations using such a model are discussed in Sec. V.

Section VI contains a discussion of the "quasi-inelastic" transition to the analog of the first excited state of the target nucleus.

II. EXPERIMENTAL METHOD AND RESULTS

The experiment was performed in a 76-cm-diam scattering chamber, using 24.6-MeV ^{3}He ions from the Oak Ridge isochronous cyclotron. The targets were enriched Ti foils ranging in thickness from 0.5 to 1 mg/cm^2. A

* Work performed under the auspices of the U. S. Atomic Energy Commission.

† Present address: Stanislaus State College, Turlock, Calif.

‡ Work done while a USAEC postdoctoral fellow under appointment of the Oak Ridge Associated Universities. Present address: University of Maryland, College Park, Md.

§ Research sponsored by the USAEC under contract with the Union Carbide Corporation.

[1] K. W. Jones, J. P. Schiffer, L. L. Lee, Jr., A. Marinov, and J. L. Lerner, Phys. Rev. **145**, B894 (1966); F. G. Perey and J. P. Schiffer, Phys. Letters **17**, 324 (1966); R. Sherr, Bull. Am. Phys. Soc. **12**, 474 (1967).

[2] C. D. Goodman, J. D. Anderson, and C. Wong, Phys. Rev. **156**, 1249 (1967).

[3] P. G. Roos, C. A. Ludemann, and Jerome J. Wesolowski, Phys. Letters **24B**, 656 (1967).

[4] A. M. Lane and J. M. Soper, Nucl. Phys. **35**, 676 (1962); A. M. Lane, Phys. Rev. Letters **8**, 171 (1962); G. R. Satchler, R. M. Drisko, and R. H. Bassel, Phys. Rev. **136**, B637 (1964); J. D. Anderson, C. Wong, J. W. McClure, and B. D. Walker, *ibid.* **136**, B118 (1964).

[5] E. H. Schwarcz, Phys. Rev. **149**, 752 (1966).

[6] V. A. Madsen, Nucl. Phys. **80**, 177 (1966).

counter telescope system, consisting of a 500-μ dE/dx silicon detector and a 1500-μ E silicon detector, was used in conjunction with a multiplier circuit and conventional electronics. The total resolution observed in the triton energy spectra was 90 keV full-width at half-maximum. Figure 1 shows the energy spectra of all five isotopes at 33°. The tallest peak in each case represents the "quasi-elastic" transition.

Differential cross sections were measured for all isotopes from 18° to 49° in the laboratory, with the exception of ^{48}Ti, for which the measurements were made out to 70°. Figure 2 shows the five angular distributions

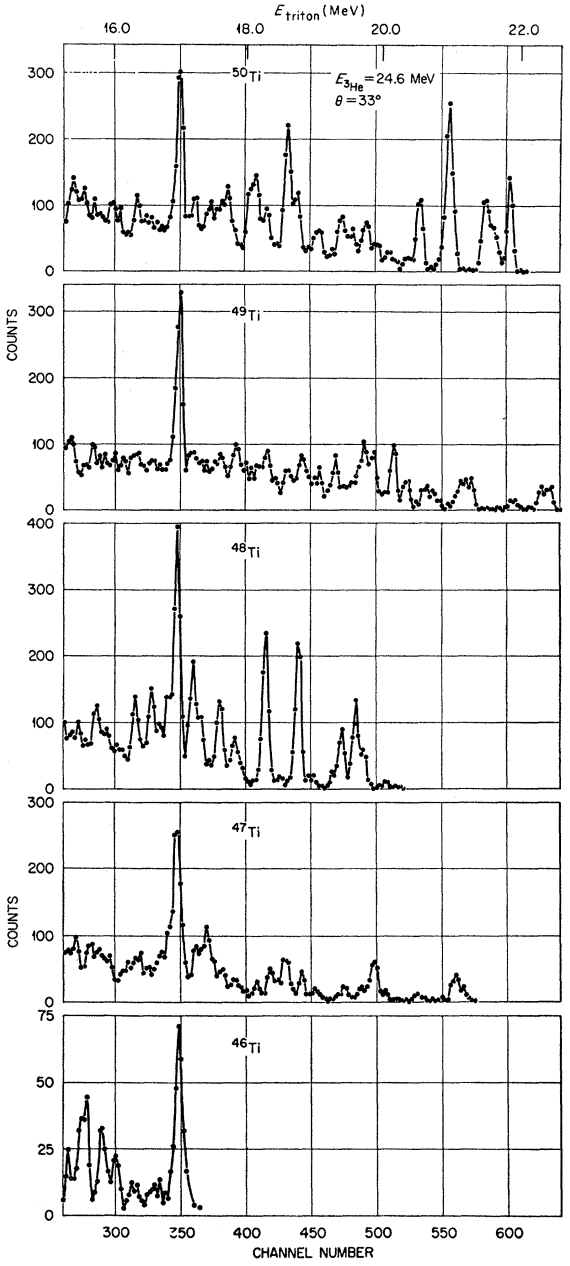

FIG. 1. Triton energy spectra for the Ti(^{3}He,^{3}H)V reaction for the Ti isotopes at 33°.

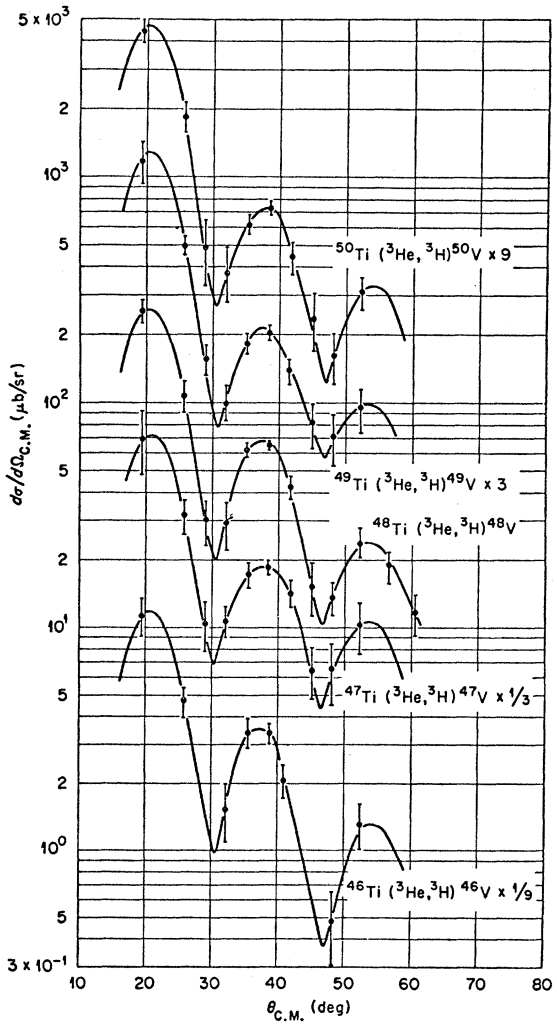

FIG. 2. Angular distribution for the analog states. The solid curves are drawn through the points for convenience in studying the data. Some of the cross sections have been offset by factors of 3 for comparison purposes.

obtained for the analog states. The only notable differences in the shapes of these distributions are an increase in the width of the maxima and a filling in of the minima for the odd isotopes, particularly for ^{47}Ti. Further discussion can be found in Ref. 3.

III. COUPLED-CHANNELS ANALYSIS

In an attempt to describe the (p,n) charge-exchange process, Lane assumed that the nucleon optical-model potential could be written in the form[7] (neglecting the spin-spin interaction in the two-body force)

$$U=U_0(r)+U_1(r)\mathbf{t}\cdot\mathbf{T}_0/A+(\tfrac{1}{2}-t_3)U_c(r), \quad (1)$$

where A is the mass number of the target, $U_0(r)$ is the usual one-channel optical potential, $U_c(r)$ is the Coulomb potential felt by a proton, $\mathbf{t}$ and $\mathbf{T}_0$ are the isobaric

[7] A. M. Lane, Phys. Rev. Letters 8, 171 (1962); Nucl. Phys. 35, 676 (1962).

spin vectors of the projectile and target nucleus, respectively, and t_3 is $+\frac{1}{2}$ for a neutron and $-\frac{1}{2}$ for a proton. When placed in the Schrödinger equation, this optical potential yields a set of coupled equations given by[4]

$$\begin{aligned}&[T+U_p+U_c-(1/2A)T_0U_1]\Psi_p\\&\qquad+(1/A)(T_0/2)^{1/2}U_1\Psi_n=0,\\&[T+U_n+\Delta_c+(1/2A)(T_0-1)U_1]\Psi_n\\&\qquad+(1/A)(T_0/2)^{1/2}U_1\Psi_p=0.\end{aligned}\tag{2}$$

The term T is the kinetic energy operator, Δ_c is the Coulomb energy difference between the target nucleus ground state and its analog, and Ψ_p and Ψ_n are proton and neutron wave functions. The one-channel optical potentials have been written in more general terms than in the original Lane equation. Thus U_p and U_n refer to the optical potentials for the incoming proton channel and the outgoing neutron channel. The (^{3}He,^{3}H) process can be described by these equations with suitable modifications to account for the Coulomb potential in the outgoing channel. This can be done by replacing $(\frac{1}{2}-t_3)$ in Eq. (1) by $(\frac{3}{2}-t_3)$, where t_3 is $+\frac{1}{2}$ for a triton and $-\frac{1}{2}$ for ^{3}He. The coupled equations then become

$$\begin{aligned}&[T+U_{^3\mathrm{He}}+2U_c-(1/2A)T_0U_1]\Psi_{^3\mathrm{He}}\\&\qquad+(1/A)(T_0/2)^{1/2}U_1\Psi_{^3\mathrm{H}}=0,\\&[T+U_{^3\mathrm{H}}+\Delta_c+U_c+(1/2A)(T_0-1)U_1]\Psi_{^3\mathrm{H}}\\&\qquad+(1/A)(T_0/2)^{1/2}U_1\Psi_{^3\mathrm{He}}=0.\end{aligned}\tag{3}$$

It should be noted that one expects the strength of the symmetry potential term U_1 to be approximately the same for the (p,n) or the (^{3}He,^{3}H) reactions. This is due to the Pauli exclusion principle, which allows only one of the protons in the ^{3}He nucleus to charge exchange and to the assumption that within an optical-model framework the nucleons in ^{3}He can be treated somewhat independently. (This is the basis of the microscopic calculations of Sec. IV.) The validity of this assumption rests on the successful comparison of various reaction data with an optical-model theory which requires a ^{3}He potential three times that of the nucleon potential. This comparison of the (^{3}He,^{3}H) and (p,n) strengths on the basis of a microscopic model is given in Sec. VI of Ref. 6.

The optical potential parameters for the incident channel were obtained by fitting ^{3}He elastic scattering data from the Ti isotopes. These data were also obtained using 24.6-MeV ^{3}He ions from the Oak Ridge isochronous cyclotron.[8] Optical-model calculations were carried out using two independent search codes, HUNTER and LOKI.[9,10] Since the shapes of both the elastic and "quasi-elastic" (^{3}He,^{3}H) angular distributions varied only slightly from isotope to isotope, we shall present only the results found for one isotope, in particular the one for which the angular distribution was carried out to the largest angle, viz., ^{48}Ti. Because no pertinent triton elastic scattering data were available, the outgoing channel optical parameters were taken to be the same as those used in the incident channel. If the outgoing triton energy were the same as the incident ^{3}He energy, this substitution would be reasonable to the extent of the validity of the charge independence of nuclear forces. In this particular experiment the outgoing triton energy was lower by approximately 7 MeV. However, Gibson *et al.*[11] have pointed out that the energy dependence of the ^{3}He optical potential appears to be quite small. The optical potential used in fitting the data had the form

$$U_{^3\mathrm{He}}(r)=-Vf(r)-i[Wg(r)+W_Dg_D(r)]+U_{\mathrm{Coul}}(r),$$

where

$$\begin{aligned}&f(r)=[1+\exp((r-R_u)/a_u)]^{-1};\quad R_u=r_uA^{1/3},\\&g(r)=[1+\exp((r-R_w)/a_w)]^{-1};\quad R_w=r_wA^{1/3},\\&g_D(r)=\frac{4\exp((r-R_w)/a_w)}{[1+\exp((r-R_w)/a_w)]^2},\end{aligned}\tag{4}$$

and $U_{\mathrm{Coul}}(r)$ is the Coulomb potential of a uniformly charged sphere of radius $1.4A^{1/3}$ F. Three optical-model fits to the elastic scattering data are shown in Fig. 3, and the parameters are given in Table I. The three sets used a Woods-Saxon shape for the real part of the potential. Set I used a Woods-Saxon imaginary part. Since the optical potential options available in the code that performed the microscopic calculations discussed in Sec. V did not include a Woods-Saxon imaginary part which had geometrical parameters different from those of the real part, the parameters of set II were generated. Although sets I and II are different, they are both of the "deep" well type, i.e., the depth of the potential is about three times that of the nucleon optical potential. It is of interest to see if two very different optical potentials, both of which give reasonable fits to the elastic data, could also give comparable (^{3}He,^{3}H) distributions. For this purpose, a radically different set of parameters of the "shallow" well type was obtained by a search using as a starting point the Gol'dberg parameters.[12] Set III is the result of this search. Analysis of one- and two-nucleon transfer reactions have shown that such "shallow" well parameters, although providing good agreement with the elastic scattering data, usually give poor agreement with the reaction data. On the other hand, good agreement with experiment can usually be obtained for inelastic scattering data by using any set of parameters which fit the elastic data. Since the ^{3}He and triton

[8] C. A. Ludemann and P. G. Roos (private communication).
[9] Code HUNTER by R. M. Drisko (unpublished).
[10] F. Bjorklund and S. Fernbach, Phys. Rev. **109**, 1295 (1958).
[11] E. F. Gibson, B. W. Ridley, J. J. Kraushaar, M. E. Rickey, and R. H. Bassel, Phys. Rev. **155**, 1194 (1967).
[12] V. Z. Gol'dberg, V. P. Rudakov, and I. N. Serikov, Zh. Eksperim. i Teor. Fiz. **47**, 571 (1965) [English transl.: Soviet Phys.—JETP **20**, 381 (1965)].

optical-model wave functions are essentially the same and we are treating the interaction within an optical-model framework, we anticipate that the "quasi-elastic" (^{3}He,^{3}H) reaction will not distinguish between sets of optical parameters which fit the elastic data.

It should be noted that the potentials $U_{^3\mathrm{He}}$ and $U_{^3\mathrm{H}}$ of Eq. (3) are separate from the symmetry terms. Therefore, in principle, the potentials obtained by fitting the elastic scattering data should have the symmetry dependence extracted before using them in the coupled equations, or to be even more exact, a simultaneous search to fit the elastic and "quasi-elastic" data should be made. Such a careful simultaneous search would not be justified here in view of the approximations discussed in the previous paragraph. Furthermore, no attempt was made to modify the one-channel potentials from those given in Table I since such modifications are only of order $T_0U_1/2A$ and hence are quite small for most cases to be discussed. Justification of this procedure was obtained by comparing the elastic scattering cross sections calculated by the coupled-channels code with the curves shown in Fig. 3. Even for extreme cases, the deviations were considered small enough to be neglected.

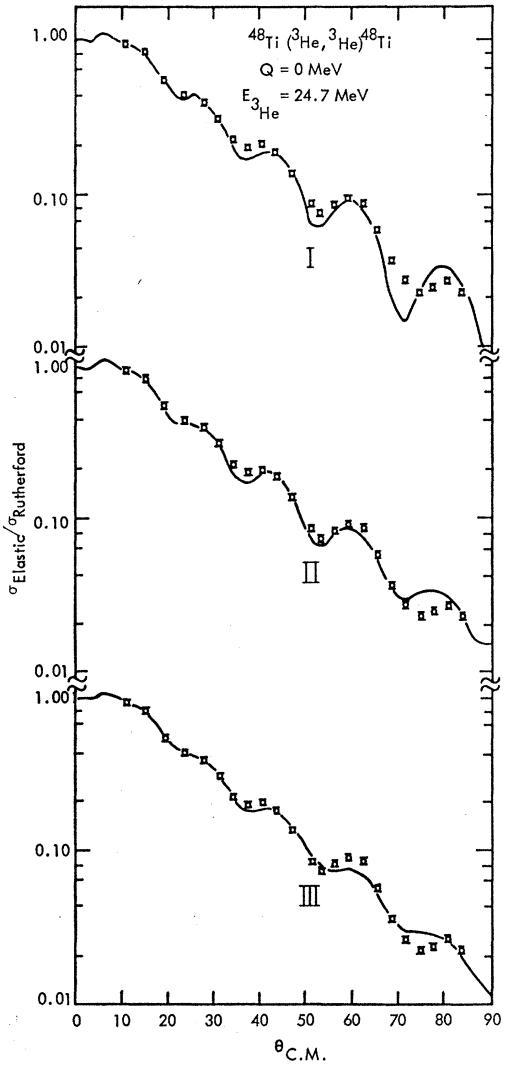

FIG. 3. Fits to the elastic ^{3}He data at 24.6 MeV for the three different sets of optical parameters listed in Table I.

TABLE I. Three sets of optical-model parameters used to fit the elastic scattering of ^{3}He from ^{48}Ti at 24.6 MeV. The Coulomb radius was taken to be equal to $1.4A^{1/3}$.

Set	V (MeV)	r_u (F)	a_u (F)	W (MeV)	W_D (MeV)	r_w (F)	a_w (F)
I	161.8	1.22	0.695	20.9	0	1.506	0.800
II	161.8	1.142	0.781	0	35.0	1.284	0.662
III	13	1.649	0.736	19	0	1.649	0.736

In solving the set of coupled equations one is faced with the choice of strength and shape for the symmetry or isobaric potential $U_1(r)$. The former is no problem since the "quasi-elastic" cross section is approximately proportional to the square of the strength of the symmetry term and hence can be obtained by the normalization of theory to experiment. There is, however, no *a priori* knowledge of what the shape should be. One is not justified in assuming that the potential has only a real part nor in assuming that the shape is the same as the one-channel optical shape.[13] However, the (p,n) analysis of Ref. 13 seems to indicate a preference for a surface symmetry term. One hopes that by fitting the angular distributions, such information can be obtained. Figure 4 shows three attempts to fit the experimental data. All three used the optical parameters of set I. For simplicity, the geometrical parameters of the symmetry term were taken to be identical to those of the optical parameters, i.e., the radius and diffuseness of the real part of the symmetry term were set equal to the radius and diffuseness of the real part of the optical potential, with a similar correspondence between the imaginary geometrical parameters. Curve a was obtained using a real symmetry term of Woods-Saxon shape. Clearly, this volume symmetry term gives poor agreement with the data. In order to normalize the calculated cross section to the data, a strength of 500 MeV was required. It should be noted that the volume potential used in Ref. 13 to fit the 18.5-MeV ^{48}Ti$(p,n)^{48}$V "quasi-elastic" data required a strength of 81 MeV. Since the strength is very dependent on the geometrical parameters used, caution must be used in making comparisons. However, in this case the (p,n) calculations were done with geometrical parameters very similar to those used to generate curve a. Hence 500 MeV is an exceptionally large strength.

Curve b is the result of using a real symmetry term of surface shape (derivative Woods-Saxon). In order to fit the magnitude of the cross section, we need

[13] G. R. Satchler, R. M. Drisko, and R. H. Bassel, Phys. Rev. 136, B637 (1964).

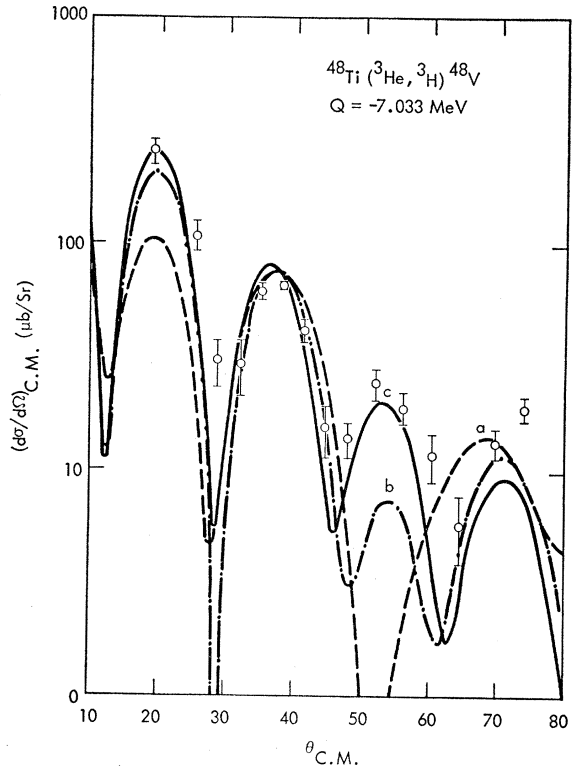

FIG. 4. Coupled-channel fits to the "quasi-elastic" data. Curve a was for a volume real symmetry term, curve b for a surface real, and curve c for a surface complex.

$U=170$ MeV, where we have defined

$$U_1^{\text{surface}}(r)=4U\frac{d}{dx}[e^x+1]^{-1};\quad x=\frac{r-R_0}{a}. \qquad (5)$$

The surface potential used in Ref. 13 to fit the ^{48}Ti$(p,n)^{48}$V data required a strength of only 72 MeV.

Curve c is also for a surface interaction but with both real and imaginary parts, each having a strength of 27 MeV. This complex surface interaction gives the best fit. It must be noted, however, that the calculation is very insensitive to the strength and shape of the real part of the potential. For example, changing the real part to a volume shape (but keeping the geometrical parameters the same) produces a result almost identical to curve c. Furthermore, setting the real strength equal to zero results in only minor changes in the theoretical curve. Such behavior is expected. Since the real potential has a smaller radius than the imaginary, one would expect the incoming particles to be absorbed before they can be influenced to any extent by the real part of the symmetry potential. To further demonstrate this, we interchanged the geometrical parameters of the real and imaginary parts of the symmetry term. With these parameters the theory was now very insensitive to the strength and shape of the imaginary part. In fact, the imaginary part could be set equal to zero with practically no change in the fit. These results are shown in Fig. 5. Lastly, a fit was generated for a real volume potential, but with geometrical parameters equal to those of the imaginary part of the one-channel optical potential. This is shown in Fig. 6. The strength in this case was 108 MeV. Although the fit is not unreasonable, it is not as good as curve c of Fig. 4. As a result of these calculations, we conclude that there is a preference for a surface symmetry term whose geometrical parameters are similar to those of the imaginary part of the one-channel potential which was used to fit the elastic scattering data, and that the strength of such a surface term is approximately 27 MeV. A direct comparison with the (p,n) results cannot be made since the calculations used different geometrical parameters. However, since both the radius and diffuseness were larger for the (^{3}He,^{3}H) case than for the (p,n) case, one expects the former calculations to require a smaller strength.

Although a complex surface interaction gave the best fit to the cross section, the fits using just a real surface (or imaginary surface) interaction with $r_0=1.506$ and $a=0.800$ were very similar. Thus, we cannot conclude from the (^{3}He,^{3}H) work that a complex symmetry term is required to fit the data. Recently Drisko *et al.* have made a comparison of the optical-model potentials for

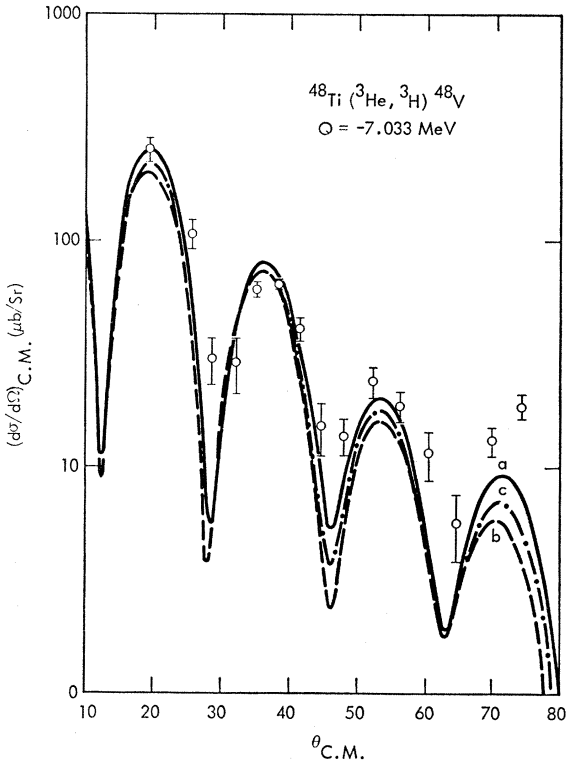

FIG. 5. Curve a is the same as curve c of Fig. 4. Curve b was obtained by interchanging the geometrical parameters of the real and imaginary parts of the symmetry term. Curve c is the same as curve b but with the imaginary part of the symmetry term set equal to zero.

^{3}He and triton elastic scattering from the same nuclei.[14] They find that the optical potential requires a symmetry term which is interpreted to be the diagonal component of the $\mathbf{t}\cdot\mathbf{T}$ term with which we are concerned here (cf. Sec. IV). The symmetry term derived in their analysis is complex. The real part is a Woods-Saxon shape of 32-MeV strength, while the imaginary part is surface (derivative Woods-Saxon) and also of 32-MeV strength. Thus the results of our (^{3}He,^{3}H) work are consistent with those of Drisko *et al.*

It was also of interest to see if good agreement with the (^{3}He,^{3}H) cross sections could be obtained using the other sets of optical parameters which also described the elastic data. Figure 7 gives the results using sets II and III of Table I. The symmetry term was taken to be identical to that used in curve c of Fig. 4. There is not much difference between these fits and those using set I (curve c, Fig. 4). Thus, as anticipated above, the particular (^{3}He,^{3}H) reaction studied here does not unambiguously differentiate between the different sets of optical parameters which gave good fits to the elastic data.

We also calculated the (^{3}He,^{3}H) cross section using set II but with the geometrical parameters of the symmetry term set equal to those of the one-channel potential of set II. This is shown in Fig. 8. The strengths

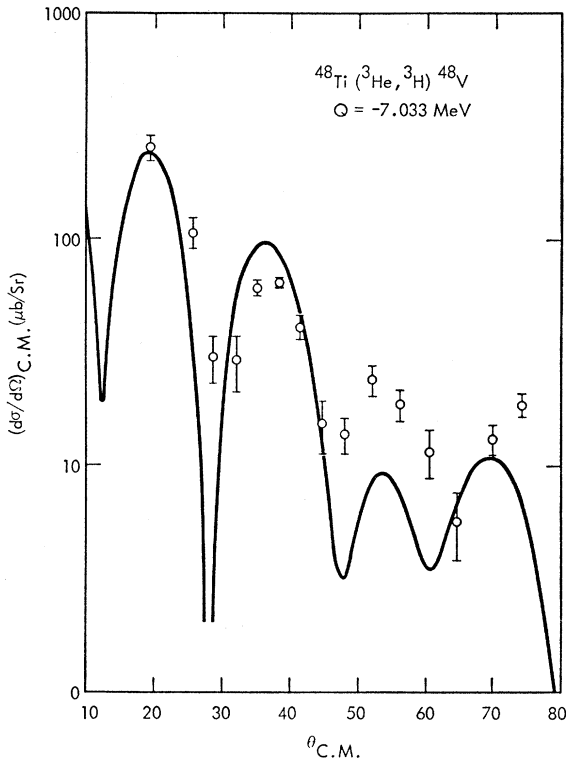

FIG. 6. Fit obtained using real volume potential of radius $1.506A^{1/3}$ and $a=0.800$.

[14] R. M. Drisko, P. G. Roos, and R. H. Bassel, in Proceedings of the International Conference on Nuclear Structure, Tokyo, Japan, 1967 (unpublished).

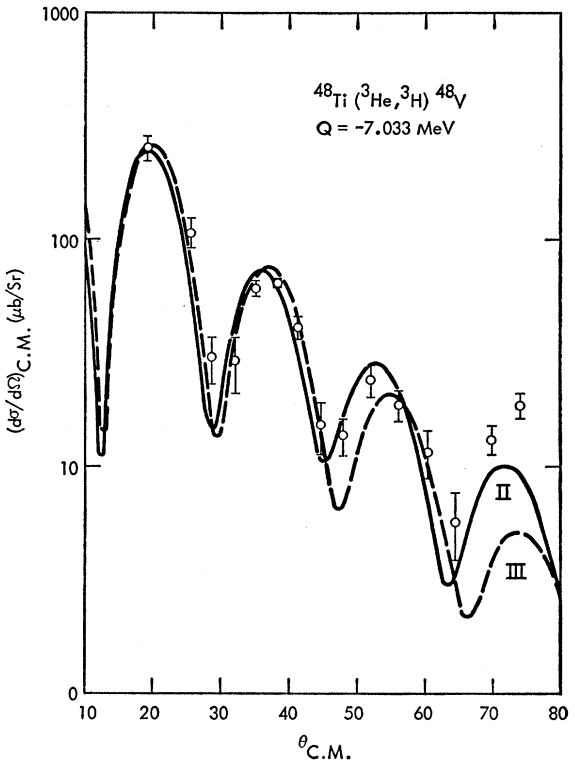

FIG. 7. ^{48}Ti(^{3}He,^{3}H)^{48}V fits using optical parameters II and III, with the same isobaric geometrical parameters as in curve 4c.

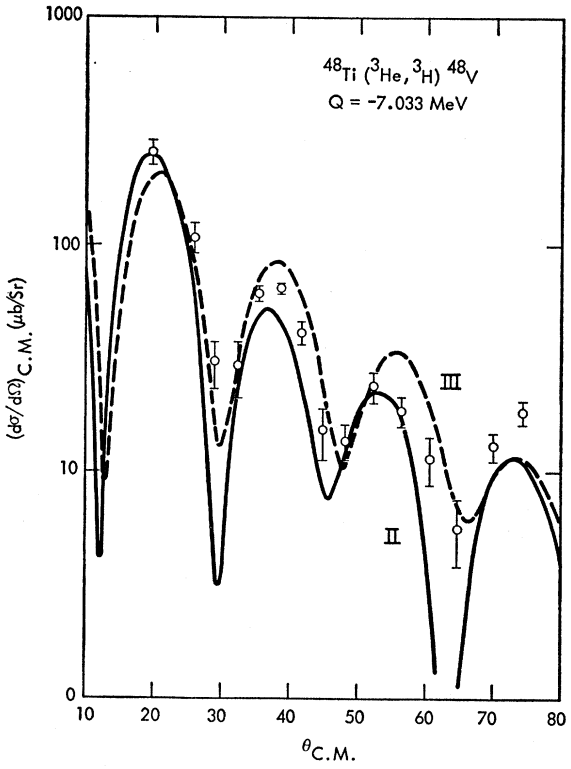

FIG. 8. ^{48}Ti(^{3}He,^{3}H)^{48}V fits using optical parameters II and III with isobaric geometrical parameters equal to the optical geometrical parameters of II and III.

of the real and imaginary symmetry terms were both set equal to 116 MeV. Similar calculations using set III are also shown in Fig. 8, where the strengths were 14.5 MeV. Both curves give reasonable results, although not as good as that of curve c of Fig. 4. Clearly the similarity of so many fits made with different sets of parameters illustrates the difficulty in obtaining a unique shape and strength for the symmetry term using just this one (^{3}He,^{3}H) reaction.

IV. COMPARISON OF DWBA AND COUPLED-CHANNEL APPROACHES

Because of the complexity of the coupled-channel solution, such codes are not always readily accessible. However, an approximation can be made to the coupled-equation approach. Satchler *et al.*[13] have shown that for reasonable well depths the off-diagonal part of the potential of Eq. (1),

$$\Delta U \equiv \langle t_3 = +\tfrac{1}{2}, T_{03} = T_0 - 1 \,|\, U \,|\, t_3 = -\tfrac{1}{2}, T_{03} = T_0 \rangle, \quad (6)$$

is very small compared to the diagonal parts,

$$\langle t_3 = \pm\tfrac{1}{2}, T_{03} = T_0 \,|\, U \,|\, t_3 = \pm\tfrac{1}{2}, T_{03} = T_0 \rangle. \quad (7)$$

The diagonal component is interpreted to give rise to the elastic scattering process and the off-diagonal component to the charge-exchange process. Thus, the latter can be treated in first-order perturbation theory, i.e., in the DWBA. Then the transition amplitude for the (^{3}He,^{3}H) reaction can be written

$$T\alpha \int d\mathbf{r}\, \chi_{^3\mathrm{H}}^{(-)*}(\mathbf{k}_{^3\mathrm{H}}, \mathbf{r}) \Delta U(r) \chi_{^3\mathrm{He}}^{(+)}(\mathbf{k}_{^3\mathrm{He}}, \mathbf{r}), \quad (8)$$

where $\mathbf{k}_{^3\mathrm{He}}$ and $\mathbf{k}_{^3\mathrm{H}}$ are the momentum vectors for the incident ^{3}He and the outgoing triton. The $\chi(\mathbf{k},\mathbf{r})$ are the distorted waves. The term $\chi_{^3\mathrm{He}}^{(+)}$ describes the elastic scattering of the ^{3}He before the charge exchange occurs and $\chi_{^3\mathrm{H}}^{(-)}$ the scattering of the triton after the reaction has taken place. Although we are primarily concerned with the "quasi-elastic" process, it should be noted that the DWBA formalism can be applied to the general charge-exchange reaction. In order to show more definitively the accuracy of the DWBA approach, cross sections were generated with code JULIE,[15] using optical-model and symmetry term parameters identical to those used in the coupled-channel approach discussed in the previous section. A comparison of the DWBA and coupled-channel fits for one such set of parameters is shown in Fig. 9. Except for a phase shift of about 1°, the two fits are almost identical.

Although caution must always be exercised when using the DWBA approach, these results indicate that in the mass and energy region being considered here and for the symmetry potentials required to fit the data the DWBA approach is a good approximation.

[15] Code JULIE by R. M. Drisko (unpublished).

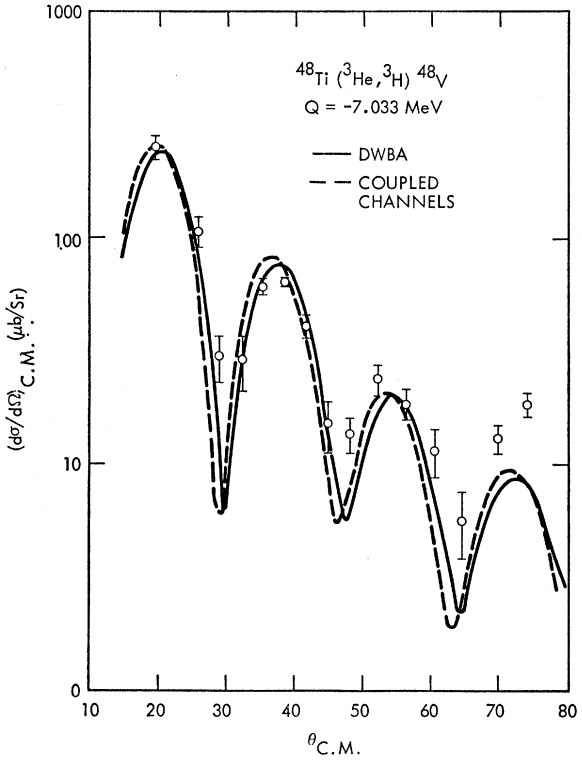

FIG. 9. Comparison of coupled-channel and DWBA fits. Dashed curve is same as curve c of Fig. 4. Solid curve is the DWBA fit using the same parameters.

V. MICROSCOPIC CALCULATIONS

Since the protons in the projectile cannot charge exchange in the "quasi-elastic" process with a neutron which is in a level whose corresponding proton level is filled, one might be tempted to view the optical-model approach discussed in the previous sections, which employs an average potential of all the nucleons, as only a phenomenological approach. However, Satchler has pointed out that since the effective two-body interaction between nucleons in nuclear matter itself depends on the difference between neutron and proton densities, all the nucleons in the nucleus contribute to the symmetry term.[13] Thus it is perhaps not surprising after all that the optical-model approach gives good agreement with the data.

A more fundamental approach to the "quasi-elastic" transition is a microscopic model. This model uses shell-model wave functions for the analog states and takes a sum of two-body forces between the projectile nucleons and target nucleons for the interaction causing the transition.[6] A number of reactions have been studied within this microscopic framework.[16] In particular, Satchler has made a rather extensive study of inelastic proton scattering and the (p,n) reaction. In the case of the (^{3}He,^{3}H) reaction, the effective interaction which

[16] G. R. Satchler, Nucl. Phys. A95, 1 (1967).

is used is the sum of nucleon-nucleon interactions between the bound nucleons in the ^{3}He projectile and the bound target nucleons. In first-order perturbation theory, the transition amplitude can be written as

$$T \propto \langle \psi_f^{(-)}(\mathbf{R}') | \Phi_f^*(\xi) \bar{V}(\mathbf{R}',\xi) \Phi_i(\xi) | \psi_i^{(+)}(R') \rangle, \quad (9)$$

where $\mathbf{R}'$ is the vector between the center-of-mass system of the projectile and that of the nucleus and ξ are all the nuclear coordinates. The $\psi^{(-)}$ and $\psi^{(+)}$ are distorted waves and the Φ is the nuclear wave function. $\bar{V}(\mathbf{R}',\xi)$ is given by

$$\bar{V}(\mathbf{R}',\xi) \equiv \sum_{i=1}^{A} \bar{V}(\mathbf{R}',\mathbf{r}_i),$$

where $\mathbf{r}_i$ is the space coordinate of the ith nucleon bound in the nucleus. $\bar{V}(\mathbf{R}',\mathbf{r}_1)$ is the effective interaction between the ^{3}He projectile and nucleon one in the nucleus.

The effective ^{3}He-nucleon interaction can be expressed in terms of the parameters of an effective nucleon-nucleon interaction in nuclear matter (cf. Appendix). Thus it is of interest to determine if the parameters of $V_{N\text{-}N}$ (the effective nucleon-nucleon interaction) needed to give agreement with (^{3}He,^{3}H) data are consistent with those obtained from comparisons with other experimental information, in particular (p,n) "quasi-elastic" data.

If a Gaussian form is chosen for $V_{N\text{-}N}$, it is shown in the Appendix that the effective ^{3}He-nucleon interaction parameters can be expressed in terms of those of $V_{N\text{-}N}$ in a trivial manner. In fact, in this case the effective ^{3}He-nucleon interaction is also a Gaussian whose strength $V_{0\beta}'$ and range parameter γ_3 are related in a simple way to the strength $V_{0\beta}{}^G$ and range parameter γ_1 of $V_{N\text{-}N}$. This is discussed in more detail in the Appendix. If a Yukawa shape is chosen for $V_{N\text{-}N}$, then the resulting expression for the ^{3}He-nucleon interaction is rather complex and is given by Eq. (A10).

Since the microscopic codes available did not allow for effective interaction shapes as complex as that given by Eq. (A10), we carried out the microscopic calculations for the ^{48}Ti(^{3}He,^{3}H)^{48}V "quasi-elastic" scattering, using both Gaussian and Yukawa shapes for the effective ^{3}He-nucleon interaction with a number of different ranges. The calculations were carried out using both the DRC[17] and ATHENA[18] code in conjunction with JULIE. We assumed pure $f_{7/2}$ wave functions for the analog states. The $f_{7/2}$ bound-state wave functions were generated in a Woods-Saxon well of radius $r_0=1.25$ F, diffuseness $a=0.65$ F, and a spin-orbit coupling of 25 times the Thomas term. The Coulomb potential from a uniformly charged sphere of radius $1.25A^{1/3}$ F was included for one proton. The well depth was adjusted

[17] W. R. Gibbs, V. A. Madsen, J. A. Miller, W. Tobocman, E. C. Cox, and L. Mowry, National Aeronautical and Space Administration Technical Note, NASA TN D-2170 (unpublished).
[18] M. B. Johnson, L. W. Owen, and G. R. Satchler, Phys. Rev. 142, 748 (1966).

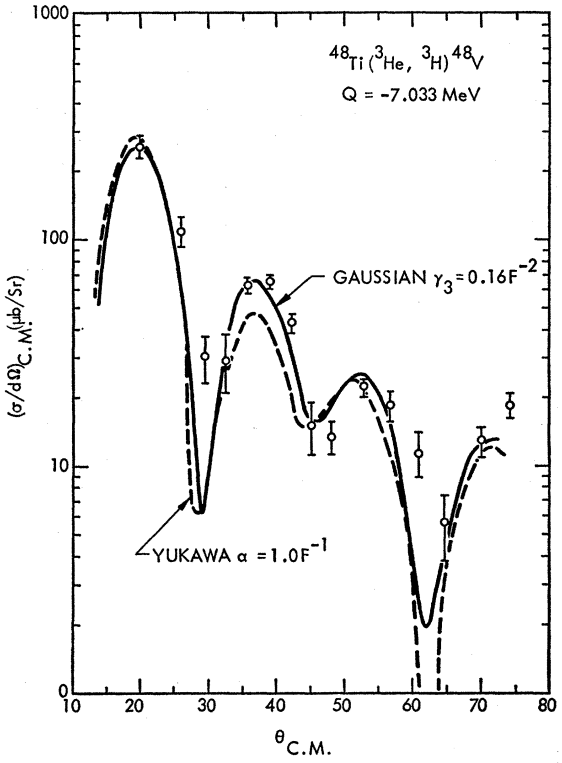

FIG. 10. Microscopic calculations using a Yukawa or a Gaussian for the effective interaction.

to give a binding energy of 8.5 MeV for the neutron and 3.82 MeV for the proton. The distorted waves were generated with the optical-model parameters of set II. From a comparison with the data, it was found that the best results using a Yukawa shape for the effective ^{3}He-nucleon interaction were obtained for a range $=1.0$ F. Using the Gaussian shape, reasonable agreement with the data was obtained for values of γ_3 ranging from 0.13 to 0.17. We chose $\gamma_3=0.16$, since this value corresponds to a value of $\gamma_1=0.25$ for the nucleon-nucleon Gaussian interaction [from Eq. (A8)] and a Gaussian of this range is equivalent to a Yukawa interaction of range $=1.0$ F to order k^2 in the Fourier transforms of the interactions. The curves for the two calculations are shown in Fig. 10, normalized with respect to the data. The strengths obtained from this normalization are listed in Table II.

To facilitate the comparison to the (p,n) results, we

TABLE II. Comparison of experimental (^{3}He,^{3}H) strengths and those expected for this reaction based on the (p,n) results.

	^{48}Ti(^{3}He,^{3}H)^{48}V			^{48}Ti(p,n)^{48}V		
Interaction	Range γ_3 or α	Experimental strength (MeV)	"Theoretical" strength (MeV)	Range γ or α	Experimental strength (MeV)	Volume integral
Gaussian	0.16	4.76	2.8	0.25	5.4	241
Yukawa	1.0	55	34	1.0	20	252

have carried out ^{48}Ti$(p,n)^{48}$V "quasi-elastic" calculations for 18.5-MeV protons using the same bound-state wave functions as in the (^{3}He,^{3}H) calculations. The optical-model parameters were taken from Satchler *et al.*[13] These calculations were done with a Yukawa interaction of range = 1.0 F and a Gaussian interaction of $\gamma_1 = 0.25$. The two calculations give almost the same angular distributions and a reasonable description of the data of Anderson *et al.*[19] The strengths obtained from a normalization to the data are listed in Table II. Also we have listed the volume integrals of the potentials for the two (p,n) calculations. Johnson *et al.*[18] suggest this as a method of comparing different potentials. As we can see, the Yukawa and Gaussian have essentially the same volume integral. It should be noted that the ^{48}Ti$(p,n)^{48}$V results are in good agreement with those obtained by Satchler for the ^{52}Cr$(p,n)^{52}$Mn "quasi-elastic" reaction at 18.5 MeV.[16] He obtained a good fit with a Yukawa of range = 1.0 F and strength = 24 MeV.

In Table II we have listed the strength expected for the (^{3}He,^{3}H) reaction based on the (p,n) results. For the Gaussian interaction we used Eq. (A6) and obtained a strength of 2.8 MeV. The experimental strength is approximately twice the strength expected, but considering the simplicity of the description for this complex interaction, we consider this reasonable agreement.

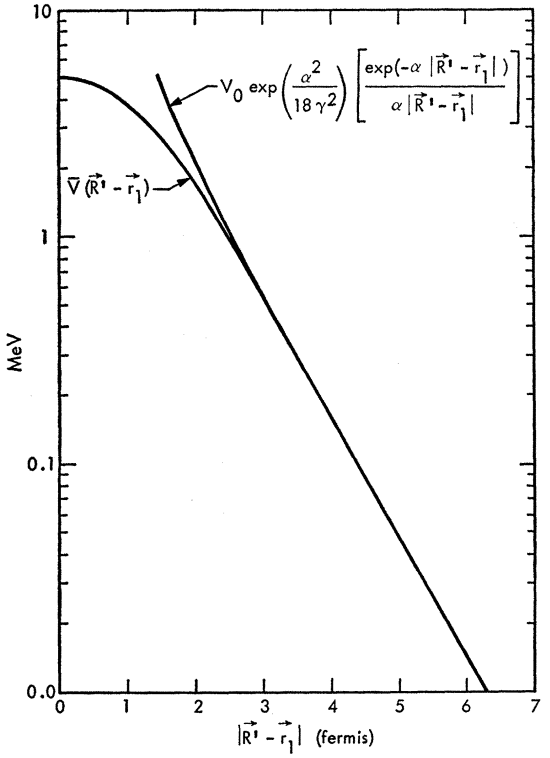

FIG. 11. Effective interaction versus separation distance.

[19] J. D. Anderson, C. Wong, J. W. McClure, and B. D. Walker, Phys. Rev. 136, B118 (1964).

The comparison of the Yukawa interactions is more difficult. Inserting the Yukawa nucleon-nucleon interaction obtained from the (p,n) calculation [range = 1.0 F and a strength of 20 MeV] into Eq. (A10) and numerically integrating, we obtain for the effective ^{3}He-nucleon interaction the curve shown in Fig. 11. This certainly does not resemble a simple Yukawa.

However, the wave functions of the nucleons are peaked inside the nuclear surface and one expects that the ^{3}He projectile is strongly absorbed inside the nuclear surface. To check the absorption, we used lower radial cutoffs in the DWBA calculation. It was found that lower cutoffs up to ~6.0 F had very little effect on the calculation. Since the density distribution for the $1f_{7/2}$ wave function is peaked far inside of 6 F, we expect that the (^{3}He,^{3}H) charge-exchange reaction will take place predominantly for large values of R (the ^{3}He-target nucleon separation). One can show that for large values of R, Eq. (A10) can be approximated by a Yukawa of range $= 1/\alpha$ given by

$$V = V_{0\beta}''[\exp(-\alpha r)]/\alpha r,$$

where

$$V_{0\beta}'' = V_{0\beta}{}^Y \exp(\alpha^2/18\gamma^2).$$

Setting $\alpha = 1$, $V_{0\beta}{}^Y = 20$ MeV, and $\gamma = 0.318$ (cf. the Appendix) in the above equation, one obtains $V_{0\beta}'' = 34$ MeV. A simple Yukawa with $\alpha = 1$ and strength = 34 MeV is plotted in Fig. 11. Beyond 3 F, the agreement between this Yukawa and the "exact" effective ^{3}He-nucleon interaction is excellent. The strength required to fit the (^{3}He,^{3}H) reaction with a Yukawa interaction of $\alpha = 1.0$ F^{-1} was ~55 MeV. Again, this is somewhat higher than the predicted 34 MeV.

Although both microscopic form factors result in strengths roughly twice that expected, the agreement seems quite reasonable, considering the great simplification of this complex reaction. One seemingly strange result is that the microscopic form factor, which describes the "quasi-elastic" scattering quite well, peaks well inside that preferred in the optical-model approach of Sec. III; viz., derivative Woods-Saxon with radius $R_0 = 1.506A^{1/3}$ F and diffusivity $a = 0.80$ F. This result is reconciled by the strong absorption of the ^{3}He projectile. In the region from which the major contributions to the cross section come, $R > 6.0$ F, the microscopic and collective form factors are essentially the same.

VI. QUASI-INELASTIC TRANSITIONS

In addition to the "quasi-elastic" scattering to the analog of the target ground state, we also have observed the transition to the analog of the first excited state of ^{48}Ti, a collective 2^+ state at 0.99 MeV. This has been conveniently described as "quasi-inelastic" scattering by Satchler *et al.*[13] Following their formalism, we describe this "quasi-inelastic" scattering by generalizing the optical potential to allow the potential to be nonspherical. This has been a highly successful method of

treating inelastic scattering to excited states. In treating "quasi-inelastic" scattering, we allow the isospin part of the potential to be nonspherical. Therefore, a quadrupole deformation of the symmetry potential excites the analog of the 0.99-MeV 2^+ state in ^{48}Ti.

As in inelastic scattering we allow the surface to be nonspherical, so that

$$R(\theta,\phi)=R_0[1+\sum_{l,m} a_{l,m}Y_l^m(\theta,\phi)].$$

Using the surface form of the symmetry potential and expanding, we obtain to first order

$$U_1(r,\theta,\phi) = -V_1'(\mathbf{t}\cdot\mathbf{T}_0/A)\left\{\frac{df}{dx}-\frac{R_0}{a}\left[\sum_{lm}\alpha_{lm}Y_l^m(\theta,\phi)\right]\frac{d^2f}{dx^2}\right\},$$

where

$$f(x)=4[1+e^x]^{-1}$$

and

$$x=(r-R_0)/a.$$

The first term in this expansion gives rise to "quasi-elastic" scattering, whereas the second term allows the "quasi-inelastic" scattering with angular momentum transfer l.

The calculation for the 2^+ analog was performed using the complex symmetry potential obtained in Sec. II. Again, as in the case of the "quasi-elastic" calculations, the imaginary part of the symmetry potential [$V_1'=27$ MeV, $R_0=1.506A^{1/3}$, $a=0.80$] completely dominates. The optical potential used was that of set I (Table I). The results of this calculation are shown in Fig. 12. The $\beta(\equiv\langle\sum_m|\alpha_{2m}|^2\rangle^{1/2})$ which was obtained by normalizing the theoretical curve to the data was $\beta=0.26$, which is in excellent agreement with the value obtained from Coulomb excitation. The β obtained from inelastic scattering of 25-MeV ^{3}He from ^{48}Ti, using both deformed real and imaginary potentials from set I, was $\beta=0.25$.[8] Thus, in contrast to the ^{56}Fe(p,n) "quasi-inelastic" scattering which gave rise to a β too large by a factor of 3–6, the (^{3}He,^{3}H) results are in excellent agreement with other measurements. However, an analysis of the (p,n) data using an optical potential with a complex symmetry term could change these results.

We also obtained an angular distribution for the analog to the 2^+ in ^{50}Ti (1.5-MeV excitation). This, too, gives the same β as obtained in other measurements. The difference between the (^{3}He,^{3}H) reaction and the (p,n) reaction to these 2^+ analogs is not understood. Satchler *et al.*[13] have pointed out that if this collective description is to be applicable, one should also see the analogs to the excited states of the odd isotopes with the quadrupole strength spread over several states. In the (^{3}He,^{3}H) reaction we see the analogs to the excited states of the odd Ti isotopes with roughly the same strength as the 2^+ analogs in the even isotopes. For example, we see the analog to the 160-keV level in ^{47}Ti$(\frac{7}{2}^-)$ and the analog to the 1.38-MeV level in ^{49}Ti$(\frac{3}{2}^-)$. Thus, for some reason, possibly the strong absorption of the mass-three projectiles, the (^{3}He,^{3}H) reaction to the analogs of excited states seems to be well described by a collective-model description.

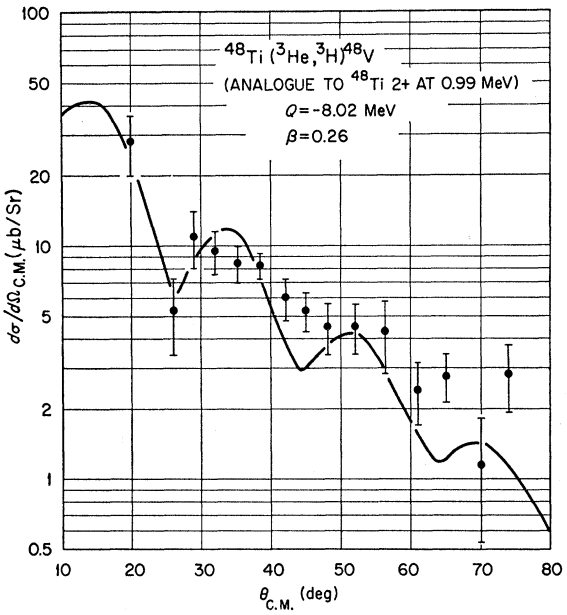

FIG. 12. Comparison of data with the predicted angular distribution for the "quasi-inelastic" (^{3}He,^{3}H) reaction to the analog of the 0.99-MeV 2+ level in ^{48}Ti.

VII. SUMMARY

The comparison of the coupled-channel calculations with the (^{3}He,^{3}H) "quasi-elastic" data indicates a preference for a surface isobaric-spin-dependent potential. Although the analysis did not unambiguously determine the shape and strength of the potential, the best agreement with the data was obtained for a complex surface potential whose strength and geometrical parameters were very similar to those obtained from an analysis of ^{3}He and ^{3}H elastic scattering data.

It was shown that the DWBA is a good approximation to the coupled-channel solution for the symmetry potential required to fit the data.

The microscopic model calculations gave good agreement with the ^{48}Ti(^{3}He,^{3}H)^{48}V data for either a Gaussian or a Yukawa nucleon-nucleon interaction and the ranges and strengths required are in reasonable agreement with those obtained from an analysis of ^{48}Ti$(p,n)^{48}$V data.

Finally, an analysis of the "quasi-inelastic" transitions to the analogs of 2^+ collective levels, using a collective-model description of inelastic scattering, required a deformability which was in excellent agreement with that obtained from other measurements.

It is clear from the success of the analysis that the (^{3}He,^{3}H) reaction is a useful probe for obtaining information about the isobaric-spin-dependent potential, the nucleon-nucleon interaction in nuclear matter, and even the quadrupole deformation.

ACKNOWLEDGMENTS

The authors wish to thank V. A. Madsen and J. D. Anderson for valuable discussions, and H. F. Lutz for the use of the Ti targets.

APPENDIX

We write the nucleon-nucleon interaction as

$$V_{N\text{-}N}=-\{V_{0\alpha}+[V_{0\beta}+V_{1\beta}\boldsymbol{\sigma}_0\cdot\boldsymbol{\sigma}_1]\mathbf{t}_0\cdot\mathbf{t}_1 +V_{1\alpha}\boldsymbol{\sigma}_0\cdot\boldsymbol{\sigma}_1\}g(\mathbf{r}_1'-\mathbf{r}_1), \quad \text{(A1)}$$

where $\mathbf{t}_0$ and $\mathbf{t}_1$ are the isospin vectors of the nucleon projectile and the target nucleon. For brevity let us consider only the ^{48}Ti "quasi-elastic" transition $0^+\rightarrow 0^+$. (An extensive discussion of the microscopic model for complex particles has been given by Madsen.[6]) In this case only the term $V_0\beta$ will contribute. When this is summed over the nucleons in ^{3}He one obtains an effective ^{3}He-nucleon interaction which can be written as

$$\bar{V}(\mathbf{R}',\mathbf{r}_1)=\int d\xi' f^2(\xi')V(\mathbf{r}_1'-\mathbf{r}_1) \equiv\int d\xi' f^2(\xi')V_{0\beta}g(\mathbf{r}_1-\mathbf{r}_1'), \quad \text{(A2)}$$

where $\mathbf{r}_1'$ is the space coordinate of the nucleon in the projectile and $f(\xi')$ is the internal space coordinate wave function of the projectile. $V(\mathbf{r}_1'-\mathbf{r}_1)$ then represents the interaction between the nucleon in the projectile and the nucleon in the target. Clearly, when the projectile is just a nucleon, $\bar{V}$ is by definition the effective nucleon-nucleon interaction.

In most microscopic analyses, the nucleon-nucleon interaction is usually taken to have either a Gaussian or a Yukawa form. If one assumes a Gaussian nucleon-nucleon interaction

$$V(|\mathbf{r}_1-\mathbf{r}_1'|)=V_{0\beta}{}^G\exp[-\gamma_1|\mathbf{r}_1-\mathbf{r}_1'|^2] \quad \text{(A3)}$$

and Gaussian wave functions for the ^{3}He and triton of the form

$$f=N\exp[-\tfrac{1}{2}\gamma^2\sum_{i<j}|\mathbf{r}_i-\mathbf{r}_j'|^2], \quad \text{(A4)}$$

where N is a normalization constant, Madsen has shown that Eq. (A2) can be integrated and also gives a Gaussian of the form[6]

$$\bar{V}(\mathbf{R}',\mathbf{r}_1)=V_{0\beta}{}^G\left(1+n\frac{\gamma_1}{\gamma^2}\right)^{-3/2}\exp\left[\frac{-\gamma_1|\mathbf{R}'-\mathbf{r}_1|^2}{1+n\gamma_1/\gamma^2}\right]. \quad \text{(A5)}$$

For ^{3}He projectiles, $n=2/9$ and $\gamma=(0.318)$.[6] We rewrite (A5) as

$$\bar{V}(\mathbf{R}',\mathbf{r}_1)=V_{0\beta}'\exp[-\gamma_3|\mathbf{R}'-\mathbf{r}_1|^2], \quad \text{(A6)}$$

where

$$V_{0\beta}'=\frac{V_{0\beta}{}^G}{[1+(2/9)(\gamma_1/(0.318)^2)]^{3/2}} \quad \text{(A7)}$$

and

$$\gamma_3=\frac{\gamma_1}{1+(2/9)(\gamma_1/(0.318)^2)}. \quad \text{(A8)}$$

Thus, the strength and range obtained for the effective projectile nucleon interaction by fitting (^{3}He,^{3}H) distributions can be compared with the strength and range for the effective nucleon-nucleon interaction as determined by fitting (p,n) distributions.

If one chooses a Yukawa interaction for $V(r_1'-r_1)$, i.e.,

$$V(\mathbf{r}_1'-\mathbf{r}_1)=V_{0\beta}{}^Y e^{-\alpha r}/\alpha r, \quad \text{(A9)}$$

then the effective interaction that results from Eq. (A2) is given by

$$\bar{V}(\mathbf{R}',\mathbf{r}_1)=V_{0\beta}{}^Y\exp\left(\frac{\alpha^2}{18\gamma^2}\right)\cdot\left\{\frac{\exp(-\alpha|\mathbf{R}'-\mathbf{r}_1|)}{\alpha|\mathbf{R}'-\mathbf{r}_1|}\left[\tfrac{1}{2}+\frac{1}{\sqrt{\pi}}\int_0^{(3\gamma/\sqrt{2})|\mathbf{R}'-\mathbf{r}_1|-\alpha/3\sqrt{2}\gamma}\exp(-y^2)dy\right]\right.$$
$$\left.+\frac{\exp(\alpha|\mathbf{R}'-\mathbf{r}_1|)}{\alpha|\mathbf{R}'-\mathbf{r}_1|}\left[-\tfrac{1}{2}+\frac{1}{\sqrt{\pi}}\int_0^{(3\gamma/\sqrt{2})|\mathbf{R}'-\mathbf{r}_1|+\alpha/3\sqrt{2}\gamma}\exp(-y^2)dy\right]\right\}. \quad \text{(A10)}$$

This clearly does not resemble a simple Yukawa. Hence, for a Yukawa, the comparison between (^{3}He,^{3}H) and (p,n) is not as simple as for the Gaussian case.